A&A 556, L1 (2013)
DOI: 10.1051/0004-6361/201321821
© ESO 2013

Astronomy & Astrophysics

Letter to the Editor

ALMA observations of the variable ^{12}CO/^{13}CO ratio around the asymptotic giant branch star R Sculptoris⋆,⋆⋆

W. H. T. Vlemmings[1], M. Maercker[2,3], M. Lindqvist[1], S. Mohamed[4], H. Olofsson[1], S. Ramstedt[5], M. Brunner[6], M. A. T. Groenewegen[7], F. Kerschbaum[6], and M. Wittkowski[3]

[1] Department of Earth and Space Sciences, Chalmers University of Technology, Onsala Space Observatory, 439 92 Onsala, Sweden
e-mail: wouter.vlemmings@chalmers.se
[2] Argelander Institute für Astronomie, Universität Bonn, Auf dem Hügel 71, 53121 Bonn, Germany
[3] European Southern Observatory, Karl Schwarzschild Str. 2, Garching bei München, Germany
[4] South African Astronomical Observatory, PO Box 9, Observatory 7935, Cape Town, Western Cape, South Africa
[5] Department of Physics and Astronomy, Division of Astronomy & Space Physics, Uppsala University, PO Box 516, 751 20 Uppsala, Sweden
[6] University of Vienna, Department of Astrophysics, Türkenschanzstraße 17, 1180 Wien, Austria
[7] Koninklijke Sterrenwacht van België, Ringlaan 3, 1180 Brussels, Belgium

Received 2 May 2013 / Accepted 30 June 2013

ABSTRACT

The ^{12}CO/^{13}CO ratio is often used as a measure of the ^{12}C/^{13}C ratio in the circumstellar environment, carrying important information about the stellar nucleosynthesis. External processes can change the ^{12}CO and ^{13}CO abundances, and spatially resolved studies of the ^{12}CO/^{13}CO ratio are needed to quantify the effect of these processes on the globally determined values. Additionally, such studies provide important information on the conditions in the circumstellar environment. The detached-shell source R Scl, displaying CO emission from recent mass loss, in a binary-induced spiral structure as well as in a clumpy shell produced during a thermal pulse, provides a unique laboratory for studying the differences in CO isotope abundances throughout its recent evolution. We observed both the ^{12}CO($J = 3 \rightarrow 2$) and the ^{13}CO($J = 3 \rightarrow 2$) line using ALMA. We find significant variations in the ^{12}CO/^{13}CO intensity ratios and consequently in the abundance ratios. The *average* CO isotope abundance ratio is at least a factor three lower in the shell (∼19) than that in the present-day (≲300 years) mass loss (>60). Additionally, variations in the ratio of more than an order of magnitude are found in the shell itself. We attribute these variations to the competition between selective dissociation and isotope fractionation in the shell, of which large parts cannot be warmer than ∼35 K. However, we also find that the ^{12}CO/^{13}CO ratio in the present-day mass loss is significantly higher than the ^{12}C/^{13}C ratio determined in the stellar photosphere from molecular tracers (∼19). The origin of this discrepancy is still unclear, but we speculate that it is due to an embedded source of UV-radiation that is primarily photo-dissociating ^{13}CO. This radiation source could be the hitherto hidden companion. Alternatively, the UV-radiation could originate from an active chromosphere of R Scl itself. Our results indicate that caution should be taken when directly relating the ^{12}CO/^{13}CO intensity and ^{12}C/^{13}C abundance ratios for specific asymptotic giant branch stars, in particular binaries or stars that display signs of chromospheric stellar activity.

Key words. stars: abundances – stars: AGB and post-AGB – stars: carbon – circumstellar matter

1. Introduction

The study of different isotope ratios provides information on the enrichment history of the interstellar medium. In particular the ^{12}C/^{13}C ratio carries an imprint of stellar evolution and nucleosynthesis, as ^{12}C is directly produced in the triple-α process, while ^{13}C is created from ^{12}C as an intermediate product of the carbon-nitrogen-oxygen (CNO) cycle. As the importance of the CNO cycle increases for more massive stars, the ^{12}C/^{13}C ratio can be used to trace the past star formation rate and stellar mass function (e.g. Prantzos et al. 1996; Greaves & Holland 1997).

Several studies have determined the photospheric ^{12}C/^{13}C ratio in evolved asymptotic giant branch (AGB) stars (e.g. Lambert et al. 1986; Ohnaka & Tsuji 1996; Abia & Isern 1997), by fitting stellar atmosphere models to photospheric lines. There have also been several papers in which the carbon isotope ratio is determined in the circumstellar envelope itself, mainly by observations of the ^{12}CO/^{13}CO ratio (e.g. Groenewegen et al. 1996; Greaves & Holland 1997; Schöier & Olofsson 2000; Milam et al. 2009). One of the main conclusions from Schöier & Olofsson (2000) is that the ^{12}CO/^{13}CO abundance ratio is a good proxy for determining the ^{12}C/^{13}C ratio provided accurate radiative transfer modeling is performed.

However, the aforementioned CO observations were all performed with single-dish telescopes, which are insensitive to spatial variations in the ^{12}CO/^{13}CO intensity ratio. The effect of, for example, an inhomogeneous circumstellar environment or (hidden) companion on the ^{12}CO/^{13}CO ratio throughout the circumstellar envelope is thus poorly known. Previous submillimeter interferometer instruments were not sensitive enough to map the often weak ^{13}CO emission at sufficient angular resolution. This has now changed with the construction of ALMA, which for the first time provides sufficient angular resolution and sensitivity to map the circumstellar ^{13}CO emission of AGB stars in detail.

⋆ Appendices are available in electronic form at http://www.aanda.org

⋆⋆ Data cubes of maps (FITS) are only available at the CDS via anonymous ftp to cdsarc.u-strasbg.fr (130.79.128.5) or via http://cdsarc.u-strasbg.fr/viz-bin/qcat?J/A+A/556/L1

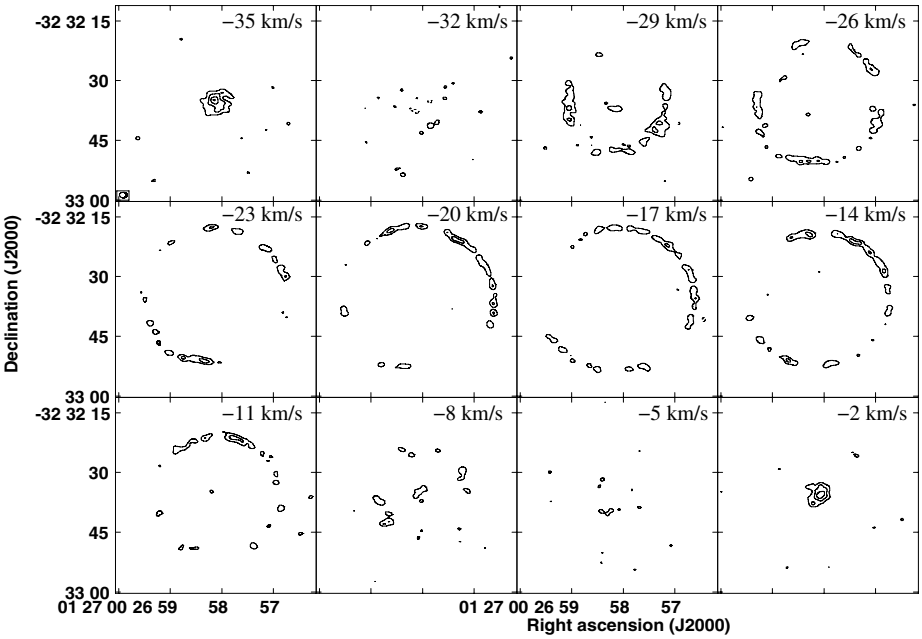

Fig. 1. ^{13}CO($J = 3 \rightarrow 2$) intensity contours. The channels are averaged over three km s^{-1}. The panels are labeled with their $V_{\rm LSR}$ and the beam is indicated in *the top left panel*. The ^{13}CO contour levels are drawn at -4σ (dashed) and $4, 8, 12$, and 16σ, with σ = 15 mJy beam^{-1}.

Here we present ^{13}CO($J = 3 \rightarrow 2$) ALMA observations of the carbon-rich AGB star R Scl located at ∼290 pc (Knapp et al. 2003). This star is one of about a dozen detached-shell sources, where the shell is thought to be created due to mass-loss modulation during a He-shell flash (i.e., a thermal pulse) (Olofsson et al. 1990). The ^{12}CO($J = 3 \rightarrow 2$) ALMA observations, taken together with the observations presented here, revealed in addition to the shell an unexpected spiral connecting the shell to the present-day ($\lesssim$300 yr) mass loss (Maercker et al. 2012, hereafter M+12). This spiral pattern is thought to be caused by the motion of a previously unknown companion at ∼60 AU from R Scl.

2. ALMA observations and results

The ^{12}CO($J = 3 \rightarrow 2$) and ^{13}CO($J = 3 \rightarrow 2$) emission lines of R Scl were observed using ALMA Band 7 (275-373 GHz) on October 3–4 and 18–19 2011 during the ALMA cycle 0 observing program. The Band 7 data contained four spectral windows of 1.875 GHz and 3840 channels each that were tuned at 345.1 GHz, 343.3 GHz, 331.1 GHz, and 333.0 GHz. This allowed us to simultaneously cover the ^{12}CO($J = 3 \rightarrow 2$) and ^{13}CO($J = 3 \rightarrow 2$) at 345.795 GHz and 330.587 GHz, respectively. The results of the ^{12}CO($J = 3 \rightarrow 2$) observations were presented in M+12 and here we focus specifically on the ^{13}CO($J = 3 \rightarrow 2$) line. The channel spacing of 0.488 MHz resulted after Hanning smoothing, in a maximum spectral resolution of 0.44 km s^{-1}. The data were taken using the cycle 0 compact configuration of ALMA, with baselines ranging from 15 m to 200 m. Using natural weighting to optimize the sensitivity for the weak ^{13}CO emission, this resulted in a beam size of 1.65″ × 1.35″ (at 330 GHz) with a position angle of 86°. A 45-point mosaic, covering a region of 50″ × 50″, was made to cover the entire shell of R Scl. The center pointing of the mosaic was taken to be the position of R Scl at $\alpha(J2000) = 01^{\rm h}26^{\rm m}58\overset{\rm s}{.}094$ and $\delta(J2000) = -32°32'35\overset{''}{.}454$. Each mosaic pointing was observed for a total of 2.42 min and the total observing time was approximately 3.8 h. The data were reduced using the Common Astronomy Software Application (CASA). After an initial correction for rapid atmospheric variations at each antenna using water vapour radiometer data and correction for the time and frequency dependence of the system temperatures, we improved the antenna positions and performed a manual delay calibration. Bandpass calibration was performed on the quasar 3C 454.3 (2.2 Jy beam^{-1}). The primary flux calibration was made using Neptune and bootstrapping to the gain calibrator J0137-245 (0.49 Jy beam^{-1}). Based on the calibrator fluxes, the absolute flux calibration has an uncertainty of ∼10%.

Imaging was then done using the CASA clean algorithm, smoothing the data to 3 km s^{-1} to detect the weak ^{13}CO($J = 3 \rightarrow 2$) emission. Similar smoothing was performed on the ^{12}CO($J = 3 \rightarrow 2$) line for a direct comparison. The rms in the emission line channels was ∼15 mJy beam^{-1} and ∼25 mJy beam^{-1} for the ^{13}CO($J = 3 \rightarrow 2$) and ^{12}CO($J = 3 \rightarrow 2$) lines, respectively. The increase in the rms noise for the ^{12}CO($J = 3 \rightarrow 2$) line is due to the complex structure of the emission (M+12). Because of the lack of short spacings, not all CO flux is recovered. Emission at scales larger than ∼15″ is resolved out. Based on single-dish observations of ^{12}CO($J = 3 \rightarrow 2$) and ^{13}CO($J = 3 \rightarrow 2$) with the APEX telescope, we estimate ∼25% of the emission is recovered for both transitions (see Appendix A). Our conclusions on the intensity ratio are thus not affected.

The ^{13}CO($J = 3 \rightarrow 2$) emission (hereafter denoted with only ^{13}CO) detected around R Scl is shown in Fig. 1. We find emission in the detached shell, for which the ^{12}CO($J = 3 \rightarrow 2$) (hereafter ^{12}CO) maps are presented in M+12. The emission has a peak flux in the shell of ∼250 mJy beam^{-1}. However, the present-day mass loss is only weakly detected (at $4\sigma \approx 60$ mJy beam^{-1}) in ^{13}CO in the $V_{\rm LSR} = -29, -11$, and -8 km s^{-1} velocity channels. Considering that the detached molecular CO shell is relatively thin, the majority of the flux will be resolved out toward the most red- and blue-shifted peaks because this is where, in projection on the sky, the shell is thickest. This can explain the relatively low level of detected ^{13}CO, as well as ^{12}CO, in the shell at $V_{\rm LSR} = -32$ and -5 km s^{-1}.

In Figs. 2 and C.1 we present the measured intensity ratio, $I_{^{12}{\rm CO}}/I_{^{13}{\rm CO}}$, around R Scl together with the contours of the ^{12}CO emission. While the ^{13}CO is not detected at all peaks of the ^{12}CO shell emission, the average $I_{^{12}{\rm CO}}/I_{^{13}{\rm CO}}$ is significantly higher in the present-day mass loss than that in the shell.

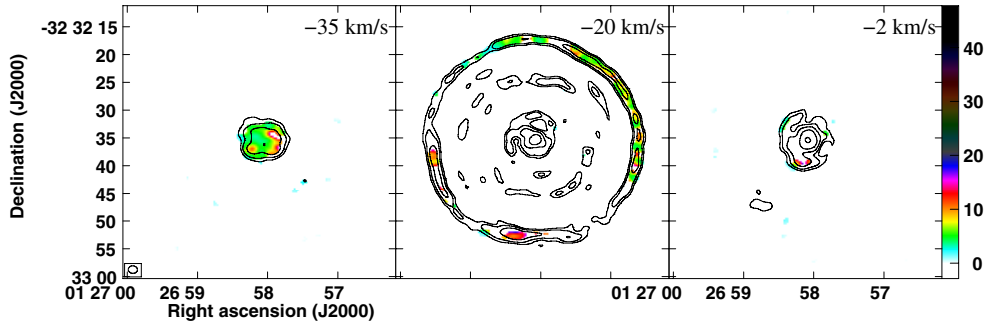

Fig. 2. Intensity ratio, $I_{^{12}CO}/I_{^{13}CO}$, (color) and ^{12}CO($J = 3 \rightarrow 2$) flux (contours) for three different velocity channels (the full channel range is presented in Fig. C.1). The channels are averaged over three km s^{-1} and the panels are are labeled according to their V_{LSR}. The ratio is presented where ^{13}CO emission is detected at higher than three σ (where σ = 15 mJy beam^{-1}) and the color scale runs from 0 to 42. The ^{12}CO contour levels are drawn at 6, 12, 24, 48 and 96σ, with σ = 25 mJy beam^{-1}. Where no ^{13}CO is detected, the contours are equivalent to a 1σ lower limit to the ^{12}CO/^{13}CO intensity ratio of 10, 20, 40, 80, and 160, respectively. The beam size is indicated in the *left panel*.

3. Discussion

3.1. The ^{12}CO/^{13}CO and ^{12}C/^{13}C ratio

If we now assume that the ^{12}CO/^{13}CO-intensity ratio is related to the ^{12}C/^{13}C ratio, we can determine the latter following Schöier & Olofsson (2000). By comparing observations of the ^{12}CO/^{13}CO line intensity ratios with the ^{12}C/^{13}C ratios derived from Lambert et al. (1986), these authors determined a correlation of the form $\frac{I(^{12}CO)}{I(^{13}CO)} = (0.6 \pm 0.2) \times \frac{^{12}C}{^{13}C}$.

Applying this relation to the average ratios found in the shell and present-day mass loss, the carbon isotope ratio of R Scl has increased from ∼12 when the detached shell was formed to ∼115 during the recent mass loss. However, these derived ratios do not take into account optical depth effects, nor effects such as selective photo-dissociation and chemical fractionation (Watson et al. 1976). In particular, the carbon isotope ratio derived for the present-day mass loss differs significantly from the value of ∼19 determined using molecular tracers in the stellar photosphere (Lambert et al. 1986)[1].

To investigate more detailed radiative transfer effects on the derived isotope ratios, we constructed radiative transfer models as described in Appendix B. The results of these are shown in Fig. 3. While our models can reproduce the double-peaked emission from the detached shell using an *average* ^{12}CO/^{13}CO ratio of 19 in the shell, the ALMA observations require a ratio higher by at least a factor of three in the present-day mass loss.

3.2. Isotope ratio in the detached shell

Our radiative transfer model can reproduce the *average* ^{12}CO/^{13}CO intensity ratio in the shell as shown in Fig. 3 for an isotope ratio unchanged from the photospheric value of 19 found by Lambert et al. (1986). However, Fig. 2 indicates that the intensity ratio ranges between as low as ∼1.5 to >40 where no ^{13}CO is detected. This requires external processes, the most likely of which are photo-dissociation and chemical fractionation. Changes in ^{12}CO/^{13}CO ratio then occur because, for photo-dissociation, self-shielding will initially allow ^{12}CO to be destroyed at a slower rate than ^{13}CO. However, at temperatures ≲35 K, chemical fractionation would favor the creation of ^{13}CO (and ^{12}C$^+$) from ^{12}CO (and ^{13}C$^+$) (e.g. Watson et al. 1976). While Mamon et al. (1988) showed that for regular

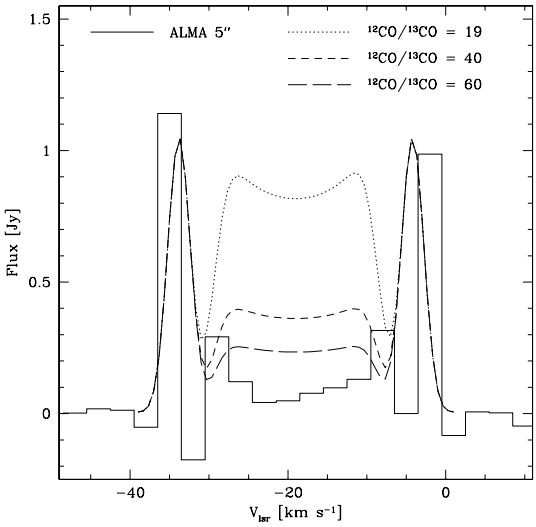

Fig. 3. Histogram of the ALMA ^{13}CO spectrum, convolved with a 5″ beam to increase the signal-to-noise ratio, along the line-of-sight to R Scl. The negative channels are due to significant missing flux near the front and back cap of the shell (see Appendix A), which does not affect the other channels with more compact emission. The dotted, short-dashed and long-dashed lines are three ^{13}CO radiative transfer models (see Appendix B) with different values for the ^{12}CO/^{13}CO ratio only in the present-day mass loss. The ratio in the detached shell is kept at 19.

AGB stars over a wide mass-loss range, the difference in ^{12}CO and ^{13}CO abundance is normally ≲20%, Bergman et al. (1993) showed that for the detached-shell source S Sct substantial fractionation is probably the explanation for the strong detection of ^{13}CO in that source. Because of the high density in the shell of R Scl, the model in Bergman et al. (1993) does not predict a significant effect from the dissociation and fractionation.

However, it is clear from Figs. 1 and 2 that the shell of R Scl is very clumpy. We find that the lowest ^{12}CO/^{13}CO intensity ratios are found to be anti-correlated with the strongest ^{12}CO peaks. This would be a natural consequence of the formation of ^{13}CO in the less dense and coldest regions (<35 K). The need for the low temperature supports our estimate of ∼50 K for the average shell temperature. We thus suggest that the CO isotope ratio variation in the shell reflects the very inhomogeneous conditions in the clumpy medium. This could further be confirmed by high-resolution observations with ALMA of, for example, the neutral carbon fine-structure lines, which should be correlated with the ^{13}CO emission peaks in the model described above.

[1] A lower ^{12}C/^{13}C ratio of ∼9 was determined in Ohnaka & Tsuji (1996). Schöier & Olofsson (2000), however, found that their sample of circumstellar ^{12}CO/^{13}CO ratios are more consistent with the work by Lambert et al. (1986).

3.3. Isotope ratio in the present-day mass loss

Our radiative transfer models furthermore indicate that the CO isotope ratio in the present-day mass loss is >60. This is in contrast with the photospheric ^{12}C/^{13}C ratio of ∼19. It implies that, contrary to the observations by Schöier & Olofsson (2000), the ^{12}CO/^{13}CO abundance ratio in the present-day mass loss of R Scl is not an accurate probe of the circumstellar ^{12}C/^{13}C ratio. Alternatively, the photospheric ^{12}C/^{13}C ratio, derived from model-fitting lines of various molecular tracers, is more uncertain as expected or is not representative for the carbon isotope ratio in the circumstellar envelope. This last possibility is difficult to reconcile with the circumstellar CO isotope observations that match the photospheric values for many sources (e.g. Schöier & Olofsson 2000; Milam et al. 2009).

Taken at face value, our results indicate a significant increase of the ^{12}C/^{13}C ratio after the detached shell was formed. Such a carbon isotope ratio increase could potentially be a direct result of the third dredge-up that occurred during the thermal pulse that created the shell. During this dredge-up, convection in the hydrogen-burning shell reaches the He-burning shell, bringing ^{12}C, created by the triple-α process, to the surface. An initial isotope abundance ratio of, in this case, ∼19, could then be increased to >40. However, this scenario is unlikely for two main reasons: 1) it would require the increased mass-loss and velocity that created the shell to occur before the ^{12}C is brought to the surface, which in current models is impossible (e.g. Stancliffe et al. 2004); and 2) it still does not explain the, in that case very recently decreased, current photospheric carbon isotope ratio of ∼19. It is thus more likely that the change in ^{12}CO/^{13}CO ratio in the present-day mass loss is due to external processes.

A speculative reason for the discrepancy between the CO and C-isotope ratios is the presence of a strong UV-radiation source within the circumstellar envelope. This source would then predominantly dissociate ^{13}CO, as ^{12}CO would be self-shielded. This strong source of UV-radiation could be the as yet undetected companion of R Scl responsible for creating the spiral structure in the shell, or it could be the active chromosphere of R Scl itself. The strength of the UV-radiation would only need to be similar to that of the interstellar radiation field and thus the UV-radiation is not necessarily expected to penetrate the entire circumstellar envelope and be directly detectable[2]. Toward the outer regions of the present-day mass-loss component, the ^{13}CO would then recombine, resulting in the observed *average* isotope ratio of ∼19 in the shell. This hypothesis could be tested by observing molecular species for which the dissociation is similar for both isotopes, such as HCN or CS. Higher-resolution observations with ALMA should also be able to determine regions in the near stellar envelope that could be shielded from UV-radiation if this radiation originates from the binary.

4. Conclusions

We found that the ^{12}CO/^{13}CO ratio in the circumstellar environment of the carbon AGB star R Scl is significantly different in the detached shell from the recent mass loss. The *average* ratio in the shell has decreased by at least a factor of three compared with the ratio of ≳60 determined for the material within <1000 AU of the central star. The ALMA observations do reveal strong variations of the ^{12}CO/^{13}CO ratio in the shell itself. These variations can very likely be attributed to the effect of isotope fractionation dominating over the dissociation by interstellar UV-radiation of ^{13}CO in the strongly clumped shell environment. However, the discrepancy between the ratio in the recent mass loss and the observed atmospheric ^{12}C/^{13}C ratio of ∼19 (Lambert et al. 1986) is puzzling. One possible explanation could be photo-dissociation of the less shielded ^{13}CO by UV-radiation from either chromospheric activity or from the thus far hidden companion that is also responsible for the previously observed spiral structure in the circumstellar envelope (M+12). In that case, one would need to conclude that the relation between ^{12}CO/^{13}CO and ^{12}C/^{13}C is not as straightforward as is often assumed. Alternatively, the photospheric ^{12}C/^{13}C ratio is not a robust indicator for the ^{12}C/^{13}C ratio of the material expelled into the interstellar medium, or uncertainties in the derived photosperic values are more significant than currently thought. More observations with ALMA that can resolve the circumstellar environment in the often much weaker ^{13}CO lines and other isotopes will be able to more firmly constrain the processes involved, while improvements in models to derive the photospheric isotope ratios are also being explored. Interestingly, if it is found that the binary companion is the cause of the CO and C isotope ratio discrepancy, such observations could also reveal hitherto hidden companions to AGB stars.

Acknowledgements. This paper makes use of the following ALMA data: ADS/JAO.ALMA#2011.0.00131.S. ALMA is a partnership of ESO (representing its member states), NSF (USA) and NINS (Japan), together with NRC (Canada) and NSC and ASIAA (Taiwan), in cooperation with the Republic of Chile. The Joint ALMA Observatory is operated by ESO, AUI/NRAO and NAOJ. W.V. was partly supported by the Deutsche Forschungsgemeinschaft (DFG; through the Emmy Noether Research grant VL 61/3-1) and by Marie Curie Career Integration Grant 321691. M.B. and F.K. acknowledge funding by the Austrian Science Fund FWF under project number P23586. We also thank the EU, Nordic and German ALMA regional centers for support during project planning and data analysis and John Black, Kjell Eriksson, Bengt Gustafsson and Richard Stancliffe for valuable discussion.

References

Abia, C., & Isern, J. 1997, MNRAS, 289, L11
Bergman, P., Carlstrom, U., & Olofsson, H. 1993, A&A, 268, 685
Greaves, J. S., & Holland, W. S. 1997, A&A, 327, 342
Groenewegen, M. A. T., Baas, F., de Jong, T., & Loup, C. 1996, A&A, 306, 241
Knapp, G. R., Pourbaix, D., Platais, I., & Jorissen, A. 2003, A&A, 403, 993
Lambert, D. L., Gustafsson, B., Eriksson, K., & Hinkle, K. H. 1986, ApJS, 62, 373
Maercker, M., Mohamed, S., Vlemmings, W. H. T., et al. 2012, Nature, 490, 232 (M+12)
Mamon, G. A., Glassgold, A. E., & Huggins, P. J. 1988, ApJ, 328, 797
Milam, S. N., Woolf, N. J., & Ziurys, L. M. 2009, ApJ, 690, 837
Ohnaka, K., & Tsuji, T. 1996, A&A, 310, 933
Olofsson, H., Carlstrom, U., Eriksson, K., Gustafsson, B., & Willson, L. A. 1990, A&A, 230, L13
Prantzos, N., Aubert, O., & Audouze, J. 1996, A&A, 309, 760
Schöier, F. L., & Olofsson, H. 2000, A&A, 359, 586
Schöier, F. L., & Olofsson, H. 2001, A&A, 368, 969
Schöier, F. L., Lindqvist, M., & Olofsson, H. 2005, A&A, 436, 633
Stancliffe, R. J., Tout, C. A., & Pols, O. R. 2004, MNRAS, 352, 984
Watson, W. D., Anicich, V. G., & Huntress, W. T., Jr. 1976, ApJ, 205, L165

Pages 5 to 6 are available in the electronic edition of the journal at http://www.aanda.org

[2] The GALEX catalog does however include a marginally significant UV-detection within ∼10″ of R Scl with a near-uv flux of ∼6 μJy.

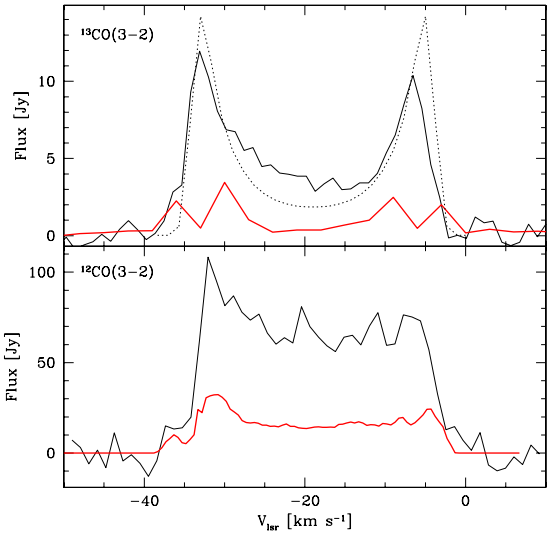

Fig. A.1. Total intensity of the ^{12}CO and ^{13}CO($J = 3 \rightarrow 2$) transitions. The solid black lines are the spectra observed with the APEX telescope in a single pointing towards the star. The solid red line is the emission detected with ALMA in an area equivalent to the APEX beam. The ^{13}CO ALMA spectrum has a velocity resolution of 3 km s^{-1}, the ^{12}CO ALMA spectrum has a velocity resolution of 0.5 km s^{-1}, and the APEX spectra have a velocity resolution of 1.1 km s^{-1}. The dotted line indicates the ^{13}CO model used to fit the ALMA observations (see text) when observed with APEX resolution. The spectra indicate that the ^{12}CO and ^{13}CO emissions are equally resolved out in the ALMA observations.

Appendix A: Comparison with single dish observations

To determine if flux losses due to insufficient uv-coverage of the ALMA observations could affect our conclusions, we compared the interferometric observations with new spectra taken with the APEX telescope. The ^{12}CO and ^{13}CO($3 \rightarrow 2$) observations were taken on Jan. 2, 2013 in a single pointing toward the star using the wobbler with a 150″ throw. The total bandwidth was 2.5 GHz, with 32768 channels, providing an initial resolution of ∼0.1 km s^{-1}, which was later averaged to ∼1.1 km s^{-1}.

The resulting spectra are shown in Fig. A.1 together with the ALMA spectra taken over an area corresponding to the APEX beam at the frequency of the CO($3 \rightarrow 2$) transition (∼19″). From this figure it is immediately obvious that a significant amount of flux is lost in the ALMA observations. We only recover approximately 25% of the total flux, indicating that the circumstellar CO has significant smooth emission over scales larger than ∼15″. Specifically in the ^{13}CO spectrum, most of the emission is lost toward the most red- and blue-shifted peaks, where, as noted above, the caps of the shell make up the largest area. A comparison of the observations with the flux of the model used to fit the ^{13}CO data, as shown in Fig. A.1 for a resolution of 19″ and in Fig. 3 for a resolution of 5″, shows that most of the small-scale flux is recovered. Considering that the present-day mass-loss extends out to <10″, the lack of ^{13}CO in the present-day mass-loss component cannot be due to the flux loss in the interferometric observations. Additionally, the single-dish comparison indicates that the ^{12}CO and ^{13}CO are similarly resolved out, 25% of the total flux is detected for both transitions, with correspondingly little effect on the observed flux ratios. We thus find that our conclusions based on the ^{12}CO and ^{13}CO intensity ratios are robust.

Appendix B: Radiative transfer modeling

To more accurately estimate the ^{12}CO/^{13}CO abundance ratio, we performed radiative transfer calculations for the CO emission using the code described in detail in Schöier & Olofsson (2001). Our model consists of two components; a present-day mass loss and a detached shell. The density, velocity and temperature of the present-day mass loss (with $\dot{M} = 3 \times 10^{-7}$ $M_{\odot}$ yr^{-1} derived from HCN modeling) are taken to be the same as described in Schöier et al. (2005), as are the stellar parameters. For the shell, we assumed a uniform gas density with a shell width of ∼400 AU and a total mass of 2.5×10^{-3} $M_{\odot}$. These parameters also match the models of M+12, although there it was found that the increased mass-loss during the thermal pulse did not decrease as rapidly as assumed here, as evidenced by the spiral of CO gas connecting the shell with the present-day mass loss. However, we do not include a description of the spiral in our models because no ^{13}CO was detected between the shell and the more recent mass loss. We furthermore assumed an average temperature of 50 K for the shell. Because no observations of higher rotational transitions of CO exist that can easily separate the emission originating in the shell from that of the present-day mass loss, the shell temperature is poorly constrained. A somewhat smaller ^{13}CO abundance and thus higher ^{12}CO/^{13}CO ratio (by ∼20%) can reproduce the observed ^{13}CO emission at higher temperatures (up to ∼70 K). Finally, we only varied the ^{12}CO and ^{13}CO abundance ratio in the present-day mass loss.

We do note that the derived ^{12}CO/^{13}CO ratio for the present-day mass-loss is different from the value of 20 derived from modeling the single-dish CO($J = 2-1$) observations (Schöier & Olofsson 2000). However, in that case it was assumed that the ratio in the shell and present-day mass loss was the same, as with the single-dish observations it is impossible to separate the two components. The CO($J = 2-1$) model also did not include the at that time unknown spiral component. If we determine the average intensity ratio over the entire envelope of R Scl from the ALMA observations, we find an intensity ratio of 10 ± 3, similar to the value of 12 measured for the CO($J = 2-1$) line (Schöier & Olofsson 2000). Furthemore, the new single-dish CO($J = 3-2$) APEX observations yield an abundance ratio similar to that found in Schöier & Olofsson (2000), because, as was the case for the CO($J = 2-1$) observations, the single-dish data cannot distinguish the detached shell and the present-day mass loss.

Appendix C: Channel maps

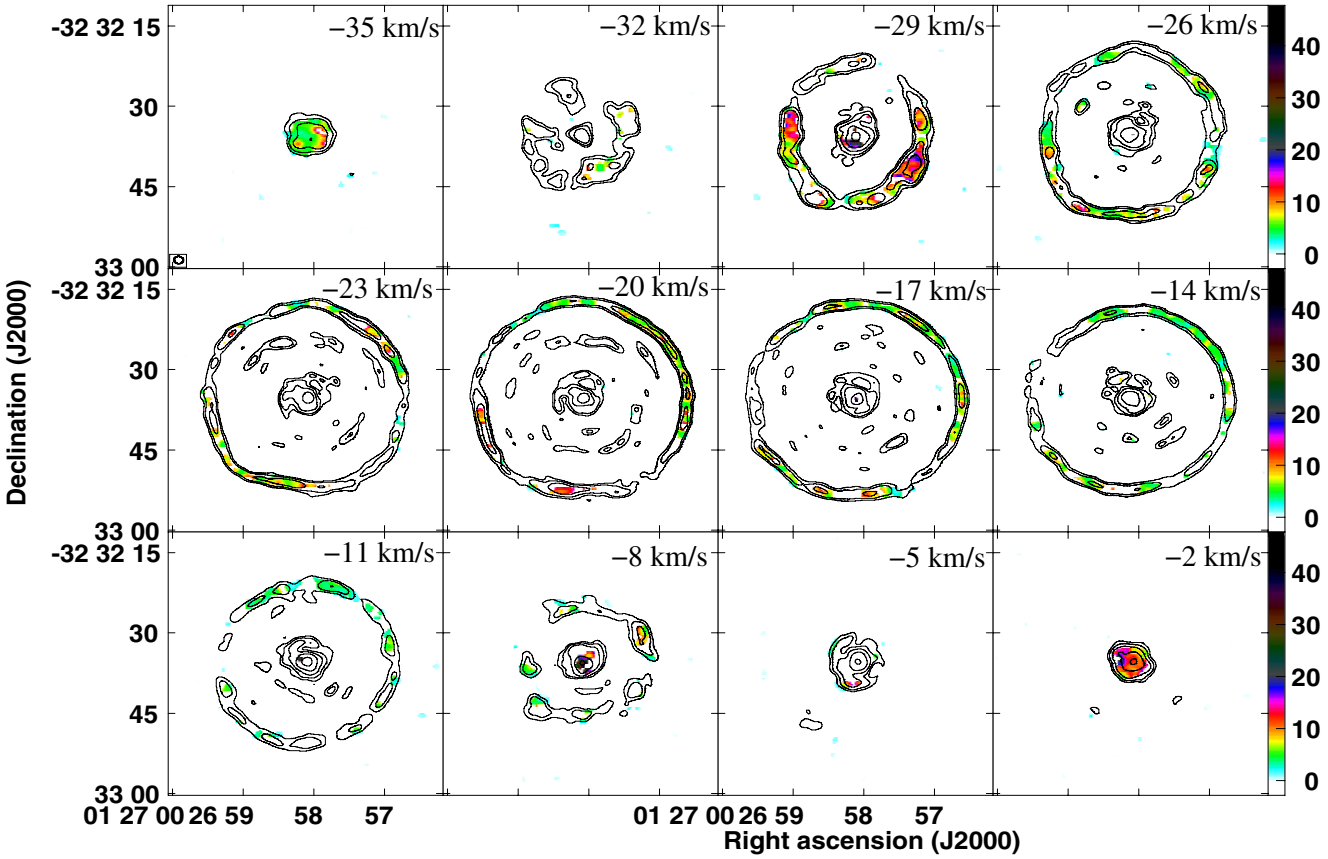

Fig. C.1. Intensity ratio, $I_{^{12}CO}/I_{^{13}CO}$, (color) and $^{12}CO(J = 3 \rightarrow 2)$ flux (contours) for the full velocity channel range. The contour and color levels are as in Fig. 2.